INTERNATIONAL JOURNAL OF PRECISION ENGINEERING AND MANUFACTURING Vol. 19, No. 12, pp. 1851-1859 DECEMBER 2018 / 1851

REGULAR PAPER

DOI: 10.1007/s12541-018-0214-9
ISSN 2234-7593 (Print) / 2005-4602 (Online)

MEMS PZT Oscillating Platform for Fine Dust Particle Removal at Resonance

Min-Geon Kim[1], Ji-Seob Choi[2], and Woo-Tae Park[1,2,#]

1 Department of Mechanical Engineering, Seoul National University of Science and Technology, 232, Gongneung-ro, Nowon-gu, Seoul, 01811, Republic of Korea
2 Department of Mechanical and Automotive Engineering, Seoul National University of Science and Technology, 232, Gongneung-ro, Nowon-gu, Seoul, 01811, Republic of Korea
Corresponding Author / E-mail: wtpark@seoultech.ac.kr, TEL: +82-2-970-6354
ORCID: 0000-0002-8330-4426

KEYWORDS: Dust removal, Micro-electromechanical systems (MEMS), PZT, Piezoelectric, Resonant frequency

Micro-electromechanical systems (MEMS) sensors designed to sense fine particles on the surface apply electrical signals to identify the corresponding physical changes on the surface. These sensors have limitations when the accumulated fine particles saturate the measurement range. In this study, we have studied how to effectively remove the accumulated particles after detection, rather than measuring the sensing performance. In general, MEMS sensors are used to detect fine particles in a high frequency region for higher resolution. However, in this work, we fabricated an oscillating platform that could be driven at a relatively low frequency region (< MHz), which the high sensing resonance. As an example of fine particles, fine dust having a diameter of 1 to 10 mm was used. The fabricated lead zirconate titanate (PZT) piezoelectric oscillating platform had a resonant frequency of 424.1 kHz, with a sensitivity of 934.2 nm/V at the resonance point. This oscillating platform was able to effectively provide sufficient acceleration to remove the dust from the surface when subjected to resonance. We have predicted the minimum required voltage to remove the particles based on van der Waals force theory, and the measured sensitivity (nm/V) of the oscillator. These values agreed to the experimentally measured voltages when the dust particles started to detach from the surface. To completely remove all the particles from the surface, the applied voltage had to be doubled.

Manuscript received: July 23, 2018 / Revised: September 17, 2018 / Accepted: September 20, 2018

1. Introduction

Over the past few decades, micro-electro-mechanical-system (MEMS) sensors have been developed for various purposes to detect the presence of particles. These MEMS sensors measured the weight of the fine particles by sensing the physical characteristics of the sensor when the fine particles are bonded to the surface of the sensor.[1-8] It is very difficult to detect the weight by static measurement because the fine particles are very small in size and weight. Instead, MEMS sensors can detect the weight dynamically because the sensor weight was small enough to change the resonant properties of the system from the addition of the fine particles. In addition, the higher the resonant frequency of the sensor, the better the sensitivity to detect the weight of the smaller particles. This is because the small percentage of the change of the resonant frequency results in larger change of the resonant frequency. In order to apply the advantages of the high resonant sensitivity of such MEMS sensors, numerous studies have been conducted to detect the weight of the particles through the changes in the resonant frequency.[5-9]

Previous studies of particle sensing can be roughly divided into two types of attachment schemes, depending on how the fine particles are bonded to the surface of the MEMS sensor. These are: (a) particles bonded chemically or biologically on the sensor surface, and (b) particles bonded physically on the surface. The chemical and biological coupling method intentionally bonds the target particles by coating a specific substance that chemically or biologically attracts and bonds on the surface of the sensor.[10-12] An example of the physical coupling method is dust particles attached to the surface. Physical coupling means that the fine particles simply sit on the surface of the sensor due to gravity and other physical attraction factors. Various physical factors, such as van der Waals attraction, electrostatic forces, and capillary attraction act between the dust particles and the surface of the sensor. Analyzing physical coupling is more complicated than the factors affecting chemical and biological binding. Numerous studies have established the practical challenges in calculating the physical coupling forces. Nevertheless, previous studies have attempted to calculate the physical adhesion through various rational assumptions.[18-21]

A representative example of physical bonding is the fine dust particles mentioned above.[13-15] A MEMS sensor that detects the weight of fine dust particles through a change in resonant frequency is resonated by various principles. The sensor resonates and detects the particles by using piezoelectric effect, thermal expansion or electrostatic force. In several studies to detect fine dust particles, the resonant frequency was reduced constantly when the dust sat on the surface of the sensor. In the case of a MEMS sensor that measures the weight of dust particles through a change in resonant frequency, it becomes more difficult to measure if the dust accumulates on the surface of the sensor and deviates from the frequency band to be measured. In addition, a study confirmed that the sensitivity of the sensor decreases as the amount of dust on the surface of the sensor increases.[15] In the recent past, a digital camera company invented a dust removal filter for Single Lens Reflector (SLR) digital cameras,[16] where they used a resonant frequency of 30-50 kHz. The shaking filter in front of the sensor shakes off the dust particles every time the camera is turned on. Other camera companies followed this approach with similar dust removal solutions.

In addition to vibration-based dust removal, there were studies using electrostatic forces. Choi et al. reported using electrostatic forces to attract and remove dust particles from the resonator surface as a self-refreshing method.[17] In solar panel developments, there were studies that used electrostatic forces to remove dust particles from the surface of a solar panel in situations where rain or wind was not available, such as space environment.[18,19] In this study, we developed a similar approach for a MEMS particle sensor. An oscillating platform that removes dust from the surface of the MEMS dust particle sensor is used to maintain the measurable frequency band, and to recover the sensitivity of the sensor to the initial state.

2. Theory

2.1 Adhesion force

The physical attraction between the fine dust particles and the surface of the sensor consists of the van der Waals attraction, electrostatic force, and attraction due to capillary action.[20-22] Van der Waals attraction is present regardless of the composition or physical shape of the material. The van der Waals force creates a strong attractive force between the particle and the surface when the distance between the particle and the surface is relatively close. The attraction due to capillary phenomenon should be considered when the fine particles contain moisture. In general, the capillary force and the electrostatic force are very small compared to the van der Waals attraction. Van der Waals force can be defined simply as Eq. (1).[23]

$$F_{ad} = F_{vdW} = \frac{AR}{6Z^2} \tag{1}$$

Where A is the Hamaker constant, R is the radius of the fine dust particle, and Z is the distance between the fine dust particle and the surface. Van der Waals attractive force has been expressed in the same way as Eq. (1) by using reasonable assumptions in various existing studies.[21,23] However, Z, which is the distance between the fine particles and the surface, is a complex parameter to measure. In reality,

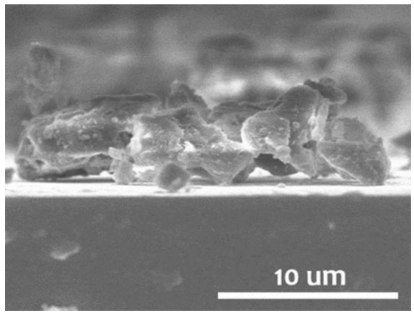

Fig. 1 Arizona ultra-fine dust particle samples on silicon wafer

the fine dust particles are not of simple spherical shape. Therefore, the value of R cannot be precisely defined. Fig. 1 is a scanning electron microscope (SEM) image of the samples of ultrafine dust particles from Arizona (ISO 12103-1, A1 Ultrafine, Powder Technology Inc.). We used these dust samples in this study.

As can be seen in Fig. 1, the shape of the fine dust particles has various shapes and it is impossible to confirm the distance between the surface and the dust particles. Since the results obtained by substituting the Hamaker constant are not always consistent with experimental data, there are errors in the estimation of van der Waals attraction expressed in Eq. (1). Due to these errors, it is not easy to accurately calculate the adhesion of the fine dust particles. Here, we make the assumption of the fine dust particles to be spherical. As such, the adhesion force between the particles and the surface can be defined as Eq. (2).[24,25]

$$F_{ad} = F_{vdW} = \sim 10^6 * F_{grav} = 10^6 * \frac{3}{4}\pi R^3 \rho g \tag{2}$$

The adhesion force of the fine dust particles defined in Eq. (2) can be expressed as Eq. (3) by separating the particle weight m_p.

$$F_{ad} = 10^6 * F_{grav} = 10^6 * \frac{3}{4}\pi R^3 \rho g = 10^6 * g * m_p \tag{3}$$

2.2 Detaching force

The dust particles attached to the surface of the vibrating sensor receive the acceleration generated by the vibration of the surface and obtain the detaching force to depart from the surface. In this case, F_{det}, which is the detaching force of the fine dust particles to be separated from the surface, is proportional to the acceleration of the surface, $a_{surface}$ and the weight of the dust particle, m_p. Therefore, the larger the weight of the particle, the greater the detaching force to be released. This relationship can be defined as Eq. (4).

$$F_{det} = a_{surface} * m_p \tag{4}$$

In Eqs. (3) and (4), we defined the adhesion force and the detaching force between the fine dust particles and the surface. When the detaching force of the dust particles defined in Eq. (4) is larger than the adhesive force, the fine dust particles can be separated from the surface, and the conditions are shown in Eq. (5). Under this condition, the minimum surface acceleration required for the fine dust particles to leave the surface can be calculated as $10^6 * g$, where g is the acceleration

Table 1 PZT oscillator design

Type	A	B
L (μm)	200	300
Total length (μm)	600	800

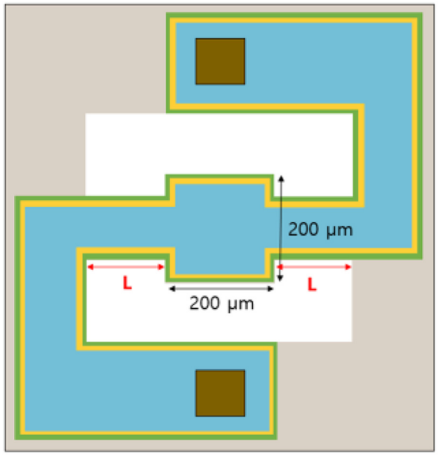

Fig. 2 Two type designs of PZT oscillating platform

due to earth's gravity. In other words, the fine dust particles can be removed from the surface if the acceleration satisfies the relation in Eq. (5) without considering the weight of the particles.

$$F_{ad} = 10^6 * g * m_p \leq F_{det} = a_{surface} * m_p \quad (5)$$

3. Design

3.1 Piezo-electric material, PZT

In MEMS, various piezoelectric materials such as AlN,[26] ZnO[27-29] and PZT[30-33] have been formed into thin films and used for various purposes. A piezoelectric material implies a substance that generates voltage when subjected to pressure or force, and this characteristic is called a piezoelectric effect. Conversely, when a voltage is applied to a piezoelectric material, the occurrence of stress in the material is called an inverse-piezoelectric effect. Because of these properties of piezoelectric materials, various MEMS devices can cause physical changes by applying electrical signals to materials, such as the AlN, ZnO and PZT. They can also detect physical changes through electrical signals. Among various characteristics of the piezoelectric material, the d_{33} coefficient indicates the displacement occurring in the same direction as the direction along which a potential difference is generated.[34-37] PZT has one of the largest values of d_{33} in comparison to other thin film piezoelectric materials. This material causes relatively large displacement when the same voltage is applied. This is the primary reason for selecting PZT in this study. Because the detaching force defined above is proportional to the acceleration of the surface. Also, the acceleration of the harmonic vibrating surface is proportional to the vibration displacement.

3.2 Oscillating platform

Applying an alternating voltage to a thin film made of a piezoelectric material can cause harmonic vibration equal to the frequency of the alternating signal. At this time, the harmonic vibration frequency and the displacement can be used to define the acceleration of the surface. If this value is larger than $10^6 * g$, the fine dust particles can be separated from the surface. Here we used a 'fixed-fixed' beam design (a bridge design with two fixed ends) to maximize our displacement while keeping the center of the platform flat during the oscillation. (Fig. 2) The center stage of the oscillator, which has the largest displacement and is most suitable for use as a sensor or actuator, is called an oscillating platform. The size of the platform was fixed to 200 × 200 (μm^2) and the length of the leg (L) connecting the platform was designed as type A and B (Table 1). In general, the resonant frequency of the beam is inversely proportional to the square of the length. Therefore, the leg designs were

Table 2 Thickness design of each layer of the oscillator

NO.	Deposition thickness from the bottom	(μm)
8	Silicon dioxide, Dielectric layer	0.2
7	Platinum, Top electrode	0.2
6	Titanium, Adhesion layer	< 5 nm
5	PZT 52/48 (lead zirconate titanate)	1.0
4	Platinum, Bottom electrode	0.2
3	Titanium, Adhesion layer	< 5 nm
2	Silicon dioxide, dielectric layer	0.2
1	Silicon nitride, back side etch stop layer	1.0

Table 3 Piezoelectric film properties (PZT 52/48)

Property	Value
d_{33} (pm/V)	295
E (GPa)	75
ρ (kg/m^3)	7500

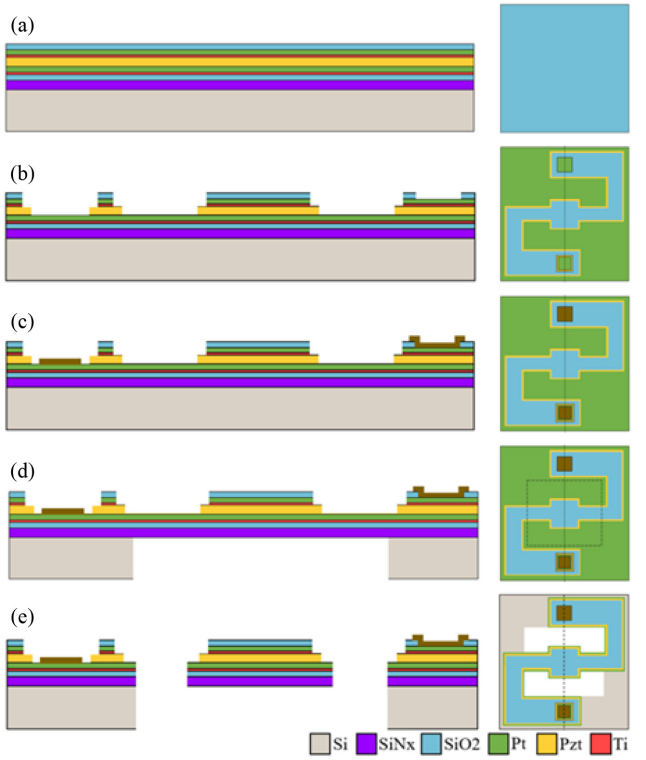

Fig. 3 Fabrication process of the PZT oscillating platform

aimed to oscillate at two close resonant frequencies. In the center of the oscillating platform, an additional MEMS sensor can be stacked. Therefore, the electrode was designed considering the space required for an additional sensor and electrodes. Thus, the upper and lower bondpads of the PZT oscillator were located far away from the oscillating platform.

4. Fabrication

The following layers were used in the fabrication of the MEMS oscillators using piezoelectric materials. The center-most layer was a layer of piezoelectric material that drives the oscillator with varying stresses when a potential difference occurs. Other layers are an electrode layer for applying an electric signal above and below the piezoelectric material, an oxide layer serving as an insulating layer, and an etch stop layer necessary for the etching process. As can be seen in Fig. 3(a), the eight layers were formed on a silicon wafer. Table 2 shows the stacking order and the thickness of each layer. The titanium layer served as an adhesive layer for the lamination of the platinum layer, which had a very small thickness. The PZT layer, which is the most important layer for driving the oscillator, was formed using a sol-gel process. The physical properties of this layer are shown in Table 3. The silicon nitride layer serves as an etch stop layer for backside etching. This nitride layer also serves as a mechanical layer to keep the piezoelectric layer asymmetric from the neutral axis. It is necessary to make the piezoelectric film asymmetric from the neutral axis to deform the structure efficiently. In Fig. 3(b), the top insulating layer, electrode layer, and piezoelectric layer were etched to form the fixed-fixed beam design. In Fig. 3(c), the pad of the oscillator electrode was deposited of gold through a lift-off process and was subsequently connected to the PCB through a wire-bonding process. In Fig. 3(d), a backside deep reactive ion etching was performed to define the oscillating region. Backside etching has the merit of accurately defining the etching region and lowering the squeeze film damping effect. However, this can suffer from inaccurate etching if there are misalignment and overetching. In Fig. 3(e), the bottom electrode, insulating layer, and silicon nitride layer was defined, and etched from the topside to completely release the structure.

Fig. 4 shows SEM images of two types of A and B PZT oscillators fabricated through the process depicted in Fig. 3. The backside etching process was used to release the PZT oscillator through the chemical etching process. Therefore, as can be seen from the image, if it is used in chemical etching, the released beam may be longer than the design stage by being excessively etched. In the initial design stage, the connection of the platform and the bridge was designed at right angles. However, in order to prevent curling of the center platform due to the residual stress from high temperature processes, the design was modified by adding a fillet. The SEM image shows that the thin film is swollen due to the poor adhesion of the PZT layer formed through the sol-gel process.

The PZT oscillating platform consists of eight layers formed on a silicon wafer on the first step of fabrication process and then patterned by sequential plasma etching. During the process of plasma etching for

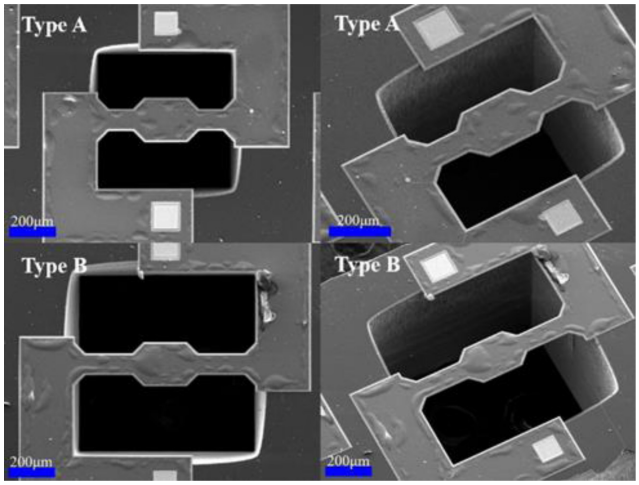

Fig. 4 SEM images of type A and B PZT oscillating platform before chip on board to PCB

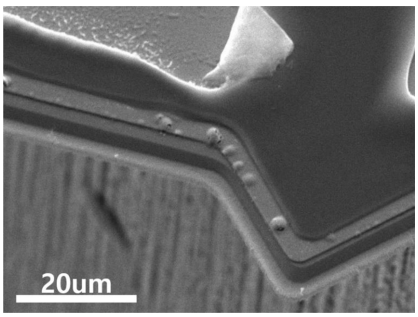

Fig. 5 Offset design to prevent short circuit between top and bottom electrode

patterning, an electrical shorting problem can occur from the re-sputtering effect between the upper and lower electrode layers of the PZT piezoelectric material. Re-sputtering implies that the molecules of the surface that are etched through the plasma etching process may migrate and stick to the periphery region. Therefore, when designing the mask for each layer, the outline of the upper electrode layer, the piezoelectric material layer, and the lower electrode layer are offset to provide space that would prevent a short circuit. The etched shape of the oscillating platform is shown in Fig. 5.

In the SEM image, the bottom electrode, the piezoelectric material, the top electrode, and the oxide layer were patterned from the bottom in accordance with the offset mask. But the oxide layer at the top is peeled off by the effect of the weakly bonded PZT layer. When the upper and lower Pt electrodes and the PZT layer are formed, deposition of SiO_2 above the proper temperature weakens the interlayer adhesion. The SiO_2 layer was deposited via a PE (plasma enhanced) process, which is a low-temperature process. But there was still some delamination. However, there was no problem in the operation of the PZT piezoelectric layer. To eliminate the delamination effect, the PZT oscillating platform can be fabricated without the oxide layer, or the active layer can be replaced with an AlN that does not depend on the high temperature process.

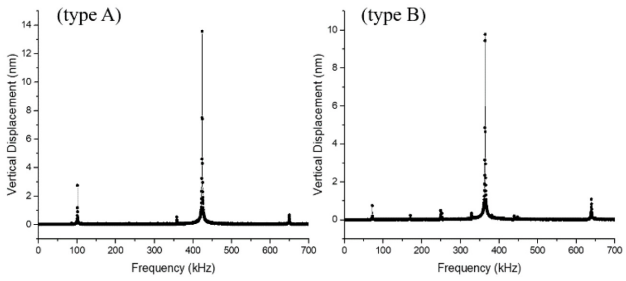

Fig. 6 The center displacement of PZT oscillating platform on frequency variation

5. Experiment

5.1 Resonant frequency measurement

A MEMS PZT oscillator die was directly connected to the PCB via wire-bonding process (COB: chip on board process). The oscillator was driven to resonate by applying an alternating voltage. Two types of PZT oscillators were designed to have different resonant frequencies. The resonant frequency was measured using a micro-system-analyzer (Polytec MSA-500). The MSA instrument can measure physical changes that occur when an electrical signal is applied to various microstructures, such as sensors, actuators, and oscillators in a specific frequency band set by the user. In this study, the mechanical displacement of the oscillating platform caused by the inverse-piezoelectric effect was measured by applying the alternating signal to the oscillator. The MSA equipment uses a laser interferometer to measure very small displacements in microscopic structures. In addition, the MSA equipment can measure the resonant frequency of a structure by applying a signal in a set frequency band, and by confirming the peak displacement point. In order to find the resonant frequency of the PZT oscillating platform, the device was driven by applying the signal in the frequency band of 0-700 kHz. The measured displacement results are shown in Fig. 6.

Theoretically, the resonant frequency has a lower value as the length of the beam becomes longer. Experimental results also showed a low resonant frequency in Type B with a longer beam length. The sensitivity of the oscillator at the resonant frequency can be defined as the measured displacement versus the applied voltage value at the driven frequency. The sensitivity thus indicates that the displacement caused by the stress change when a unit potential difference is generated across the PZT material layer. In addition, it is possible to linearly predict the displacement caused by any applied voltage. Table 4 shows the sensitivity at the resonant frequency identified in Fig. 6.

5.2 Sensitivity and surface acceleration

As shown in Eq. (5), the acceleration of the resonant surface must be greater than $10^6 * g$ in order for the fine dust particles to depart from the surface. Using the previously defined sensitivity (S) of the oscillator surface, the effective voltage value (V_{rms}) of the applied signal, and the resonant frequency (f), the displacement of the surface can be calculated using Eq. (6). However, this harmonic vibration displacement of the oscillator does not take into account of the damping effect caused by the surrounding air.

Table 4 PZT oscillator properties on resonant frequency

Type	Resonance Frequency (kHz)	Voltage (mV)	Displacement (nm)	Sensitivity (nm/V)
A	424.1	14.527	13.571	934.2
B	364.4	15.730	9.767	620.9

Table 5 Theoretical minimum voltage for fine dust removal

Type	V_{rms} [V]	V_p [V]	V_{pp} [V]
A	1.479	2.091	4.183
B	3.014	4.262	8.523

$$Displacement, d = (S)(V_{rms}) \cdot \sin(2\pi f * t) \tag{6}$$

$$Acceleration, a = (S)(V_{rms})(2\pi f)^2 \cdot \sin(2\pi f * t) \tag{7}$$

By differentiating the displacement Eq. (6) twice, the acceleration of the PZT oscillating platform can be expressed as (7). The maximum acceleration of the oscillator surface can be expressed as (8).

$$a_{max} = (S)(V_{rms})(2\pi f)^2 \tag{8}$$

By measuring the sensitivity and resonant frequency of the PZT oscillator, the maximum acceleration occurring on the surface of the oscillating platform can be calculated using Eq. (8). Through the relationship Eq. (5), it can be predicted that if the maximum acceleration value of the oscillator surface is larger than $10^6 * g$, the fine dust particles are removed from the surface. Using the sensitivity and resonant frequencies shown in Table 4, and by calculating V_{rms} as an unknown quantity, it is possible to predict the minimum applied voltage required to remove fine dust particles from the surface. Since an alternating signal is used, V_{rms} is calculated, and since the signal generator used in the experiment inputs V_{pp} value, the values are theoretically predicted as shown in Table 5.

5.3 Dust removal performance test

5.3.1 Setup

To evaluate the fine dust removal performance of two types of PZT oscillating platform in real time, we constructed a setup as shown in Fig. 7. The oscillator is monitored under an optical microscope and is driven using a signal generator. The images and video were recorded using a microscope capture software. In order to place the dust particles on the surface of the oscillator as if the fine dust naturally sits on the surface, a simple chamber was built separately to spread the dust in the air and then allowing them to slowly fall on the surface of the sensor. By placing the fine dust particles on the surface of the PZT oscillator, it is possible to reproduce the situation of the surface of the sensor that is saturated and is out of the measurable frequency band. The fine dust particles were obtained from Arizona's ultra-fine dust sample. The diameter of the fine dust particles was about 1-10 μm and the density was about 500 kg/m^3.

Since the resonant frequencies all the PZT oscillators were not perfectly matched due to the fabrication process error, it is difficult to resonate properly if the frequency of the alternating signal is set to a fixed value. Therefore, we used the sweeping frequency function of the signal generator to apply the signal within a sufficient band including

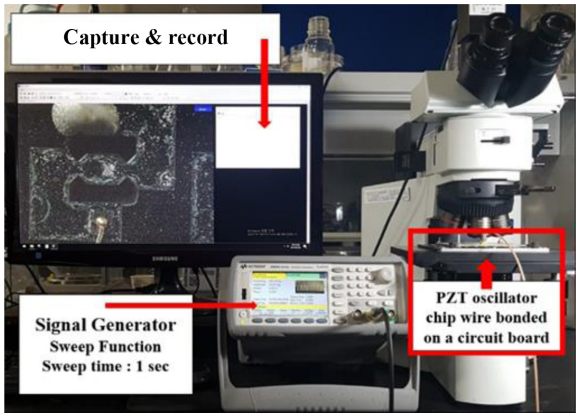

Fig. 7 Test setup to evaluate the dust removal performance of PZT oscillator

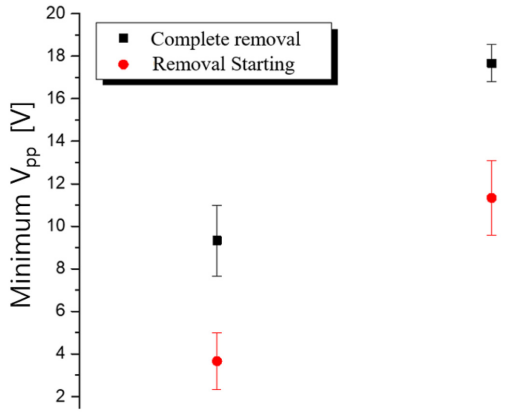

Fig. 8 The PZT oscillator's minimum required voltage for start of removal and complete removal

the resonant frequency found from the MSA equipment. For example, the resonant frequency of Type A was 424.1 kHz at the MSA equipment, and the interval set at the signal generator was 400 to 450 kHz.

5.3.2 Qualitative dust removal performance test

The setup in Fig. 7 was used to observe the micro dust removal performance of two types of PZT oscillating platforms. The voltage applied to both types of PZT oscillators was set at 20 V (V_{pp}), which was the maximum voltage of the signal generator, and the frequency of the signal was applied using the sweep function within a band inclusive of the resonant frequency. First, the results of the dust removal test of type A PZT oscillating platform are shown in Fig. 9.

For type A oscillator, it took about 2 seconds to completely remove all the dust particles from the surface of the platform. In the design phase, the PZT oscillating platform was designed to maximize the displacement and acceleration at the center of the platform when resonating. The expected experimental result was that the fine dust particles preferentially removed at the center of the platform with the greatest acceleration. However, when the type A PZT oscillator started to be driven at the resonant frequency band, first the fine dust particles gathered in a swirling motion toward the center. After a short time (~ 2.0 sec), the swirl created by the fine dust particles became smaller and the dust particles were completely removed from the center. In Fig. 10, the process of removing the fine dust particles from the type B PZT oscillating platform also showed a similar behavior as that of the type A oscillator.

Table 6 Minimum voltage measured and expected for dust removal

Type	Experimental Removal Starting V_{pp} [V]	Experimental Complete Removal V_{pp} [V]	Table 5 Estimated V_{pp} [V]
A	3.7	11.3	4.183
B	9.3	17.7	8.523

The fine dust removal time of B type oscillator was 1.2 seconds faster than the A type, but the amount of fine dust sitting on the PZT oscillating platform could be controlled in the current experimental configuration. Therefore, the removal time performance of the two types of oscillators cannot be compared with the removal time of fine dust.

5.3.3 Quantitative dust removal performance test

The two types of PZT oscillating platforms have different sensitivities, as shown in Table 4. Table 5 shows the predicted voltages required to remove the dust particles from each type of platform using this sensitivity value and the resonant frequency. In order to compare the predicted voltage with the experimentally measured voltage value, the movement of the fine dust particles on the platform surface was monitored while increasing the input voltage (V_{pp}) of the signal generator from the minimum value by 0.5 [V]. The observed results are shown in Fig. 8, which is represented by using two voltage values. The removal-starting voltage indicates the minimum voltage at which the fine dust particles start to move on the platform surface, and the complete-removal voltage indicates the minimum voltage at which the fine dust particles completely detach from the surface. Considering only the van der Waals force in the adhesion between the fine dust particles and the surface as in the above-mentioned theory, the fine dust particles must be removed at the same time regardless of the weight of the particles. However, as can be seen in Fig. 8, the fine dust particles have different time intervals of detachment from the surface. Therefore, in addition to the van der Waals attraction, adsorption by moisture capillary force and electrostatic force should also be considered in the attraction between the fine dust particles and the surface.

Since the sensitivity of type A is better than that of type B, and the resonant frequency is also larger, the result of Eq. (8) can be satisfied with a value of 6 g at a relatively low voltage value. Table 6 shows the removal-starting voltage and the complete-removal voltage observed through the experiment and compared with the values predicted in Table 5. Though it differs from the voltage at which the dust is completely removed, the predicted voltage value is similar to the voltage at which the dust particles begin to move on the surface.

6. Conclusion

In this study, resonance was used to remove fine dust particles attached to a MEMS device surface. Both types of PZT oscillating

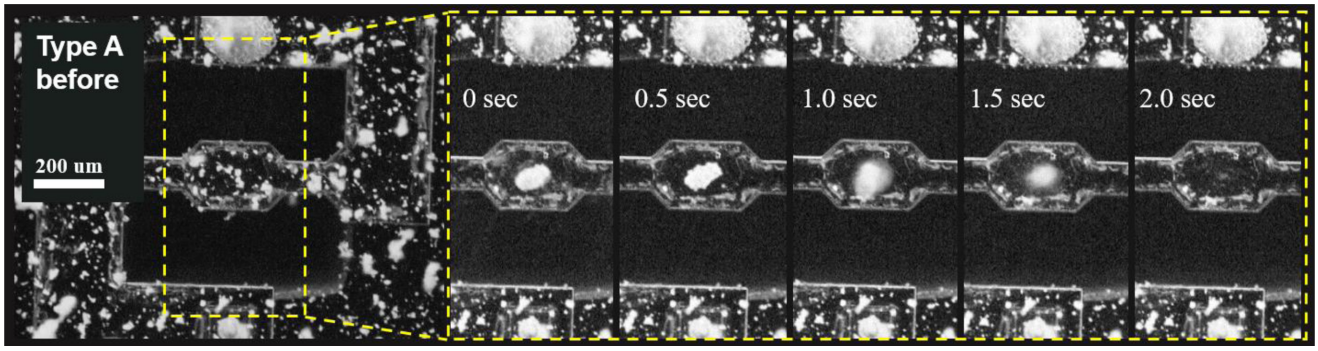

Fig. 9 Fine dust particles removal performance of type A PZT oscillating platform, sweep frequency: 400-450 kHz, V_{pp}: 20 V, sweep time: 1 sec, dust removal time: 2.00 sec

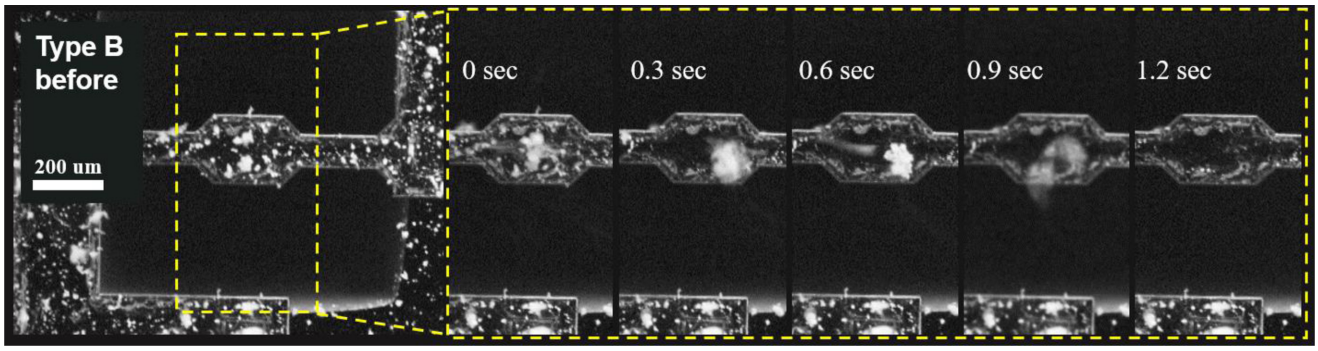

Fig. 10 Fine dust particles removal performance of type B PZT oscillating platform, sweep frequency: 350-400 kHz, V_{pp}: 20 V, sweep time: 1 sec, dust removal time: 1.20 sec

platforms could produce sufficient acceleration to remove the fine dust particles through resonance, though they perform differently. The resonance is caused by the reverse-piezoelectric effect of the PZT piezoelectric material, and the sensitivity can be defined by the resonance displacement measured by the MSA instrument and the applied voltage. It is confirmed that the sensitivity is inversely proportional to the minimum voltage required for dust removal. We have assumed surface adhesion by considering van der Waals attraction only among the factors that constitute the attraction force between the fine dust particles and the surface. Based on this, the voltage required to remove the fine dust particles was calculated and compared with the measured values. It was found that the theoretically predicted value was similar to the value at which the dust begins to move on the surface. However, it was insufficient to completely remove the dust. In conclusion, it can be stated that, it is difficult to fully predict the adhesion force between the fine dust particles and the surface by van der Waals force alone. However, it has been confirmed that by using resonance the fine dust particles can be sufficiently accelerated and removed from the surface.

ACKNOWLEDGEMENT

This work was supported by grant No. 10070100 from the Industrial Source Technology Development Programs of the MOTIE (Ministry of Trade, Industry and Energy), Korea. The authors would like to express deep gratitude for the fabrication help from MEMS Solutions and characterization help from Prof. Hongsoo Choi's lab at DGIST.

REFERENCES

1. Patolsky, F., Zheng, G., and Lieber, C. M., "Nanowire-Based Biosensors," American Chemical Society, pp. 4260-4269, 2006.
2. Datar, R., Kim, S., Jeon, S., Hesketh, P., Manalis, S., Boisen, A., and Thundat, T., "Cantilever Sensors: Nanomechanical Tools for Diagnostics," MRS Bulletin, Vol. 34, No. 6, pp. 449-454, 2009.
3. Braun, T., Barwich, V., Ghatkesar, M. K., Bredekamp, A. H., Gerber, C., Hegner, M., and Lang, H. P., "Micromechanical Mass Sensors for Biomolecular Detection in a Physiological Environment," Physical Review E, Vol. 72, No. 3, Paper No. 031907, 2005.
4. Park, B., Hong, J., and Lee, S.-B., "Real-Time Detection of Airborne Dust Particles Using Paddle-Type Silicon Cantilevers," Journal of Vacuum Science & Technology B: Microelectronics and Nanometer Structures Processing, Measurement, and Phenomena, Vol. 27, No. 6, pp. 3120-3124, 2009.
5. Yang, Y.-T., Callegari, C., Feng, X., Ekinci, K. L., and Roukes, M. L., "Zeptogram-Scale Nanomechanical Mass Sensing," Nano Letters, Vol. 6, No. 4, pp. 583-586, 2006.
6. Li, M., Tang, H. X., and Roukes, M. L., "Ultra-Sensitive NEMS-

Based Cantilevers for Sensing, Scanned Probe and Very High-Frequency Applications," Nature Nanotechnology, Vol. 2, No. 2, pp. 114-120, 2007.

7. Jensen, K., Kim, K., and Zettl, A., "An Atomic-Resolution Nanomechanical Mass Sensor," Nature Nanotechnology, Vol. 3, No. 9, pp. 533-537, 2008.
8. Ilic, B., Craighead, H. G., Krylov, S., Senaratne, W., Ober, C., and Neuzil, P., "Attogram Detection Using Nanoelectromechanical Oscillators," Journal of Applied Physics, Vol. 95, No. 7, pp. 3694-3703, 2004.
9. Eom, K., Park, H. S., Yoon, D. S., and Kwon, T., "Nanomechanical Resonators and their Applications in Biological/Chemical Detection: Nanomechanics Principles," Physics Reports, Vol. 503, Nos. 4-5, pp. 115-163, 2011.
10. Waggoner, P. S. and Craighead, H. G., "Micro- and Nanomechanical Sensors for Environmental, Chemical, and Biological Detection," Lab on a Chip, Vol. 7, No. 10, pp. 1238-1255, 2007.
11. Goeders, K. M., Colton, J. S., and Bottomley, L. A., "Microcantilevers: Sensing Chemical Interactions Via Mechanical Motion," Chemical Reviews, Vol. 108, No. 2, pp. 522-542, 2008.
12. Wu, G., Datar, R. H., Hansen, K. M., Thundat, T., Cote, R. J., and Majumdar, A., "Bioassay of Prostate-Specific Antigen (PSA) Using Microcantilevers," Nature Biotechnology, Vol. 19, No. 9, pp. 856-860, 2001.
13. Hajjam, A., Wilson, J. C., and Pourkamali, S., "Individual Air-Borne Particle Mass Measurement Using High-Frequency Micromechanical Resonators," IEEE Sensors Journal, Vol. 11, No. 11, pp. 2883-2890, 2011.
14. Thomas, S., Villa-López, F. H., Theunis, J., Peters, J., Cole, M., and Gardner, J. W., "Particle Sensor Using Solidly Mounted Resonators," IEEE Sensors Journal, Vol. 16, No. 8, pp. 2282-2289, 2016.
15. Hajjam, A., Wilson, J. C., Rahafrooz, A., and Pourkamali, S., "Detection and Mass Measurement of Individual Air-Borne Particles Using High Frequency Micromechanical Resonators," Proc. of IEEE Sensors, pp. 2000-2004, 2010.
16. Takizawa, H., Kawai, S., and Kobayashi, M., "Camera and Image Pickup Device Unit Used Therefor Having a Sealing Structure between a Dust Proofing Member and an Image Pick up Device," US Patent, 7324148B2, 2008.
17. Choi, E., Lee, S.-B., Park, B., and Sul, O., "Self-Refreshing Characteristics of an Airborne Particle Sensor Using a Bridged Paddle Oscillator," Journal of the Korean Physical Society, Vol. 68, No. 10, pp. 1170-1175, 2016.
18. Sayyah, A., Crowell, D. R., Raychowdhury, A., Horenstein, M. N., and Mazumder, M. K., "An Experimental Study on the Characterization of Electric Charge in Electrostatic Dust Removal," Journal of Electrostatics, Vol. 87, pp. 173-179, 2017.
19. Kawamoto, H. and Shibata, T., "Electrostatic Cleaning System for Removal of Sand from Solar Panels," Journal of Electrostatics, Vol. 73, pp. 65-70, 2015.
20. Ranade, M. B., "Adhesion and Removal of Fine Particles on Surfaces," Aerosol Science and Technology, Vol. 7, No. 2, pp. 161-176, 1987.
21. Shin, W., An, J., Kim, J., and Jeong, H., "Determination of Adhesion Force of Particles on Substrate Surface Using Atomic Force Microscopy," Proc. of International Conference on Planarization/ CMP Technology (ICPT 2012), pp. 1-6, 2012.
22. Salazar-Banda, G., Felicetti, M., Gonçalves, J., Coury, J., and Aguiar, M., "Determination of the Adhesion Force between Particles and a Flat Surface, Using the Centrifuge Technique," Powder Technology, Vol. 173, No. 2, pp. 107-117, 2007.
23. Corn, M., "The Adhesion of Solid Particles to Solid Surfaces, I. A Review," Journal of the Air Pollution Control Association, Vol. 11, No. 11, pp. 523-528, 1961.
24. Qi, Q. and Brereton, G. J., "Mechanisms of Removal of Micron-Sized Particles by High-Frequency Ultrasonic Waves," IEEE Transactions on Ultrasonics, Ferroelectrics, and Frequency Control, Vol. 42, No. 4, pp. 619-629, 1995.
25. Hamaker, H., "The London — Van Der Waals Attraction between Spherical Particles," Physica, Vol. 4, No. 10, pp. 1058-1072, 1937.
26. Dubois, M.-A. and Muralt, P., "Measurement of the Effective Transverse Piezoelectric Coefficient $E_{31,f}$ of AlN and $Pb(Zr_x, Ti_{1-x})O_3$ Thin Films," Sensors and Actuators A: Physical, Vol. 77, No. 2, pp. 106-112, 1999.
27. DeVoe, D. L. and Pisano, A. P., "Surface Micromachined Piezoelectric Accelerometers (PiXLs)," Journal of Microelectromechanical Systems, Vol. 10, No. 2, pp. 180-186, 2001.
28. DeVoe, D. L., "Piezoelectric Thin Film Micromechanical Beam Resonators," Sensors and Actuators A: Physical, Vol. 88, No. 3, pp. 263-272, 2001.
29. Han, C.-H. and Kim, E. S., "Micromachined Piezoelectric Ultrasonic Transducers Based on Parylene Diaphragm in Silicon Substrate," Proc.of Ultrasonics Symposium, pp. 919-923, 2000.
30. Ren, T.-L., Zhu, Y.-P., Yang, Y., Wu, X.-M., Zhang, N.-X., et al., "Micro Acoustic Devices Using Piezoelectric Films," Integrated Ferroelectrics, Vol. 80, No. 1, pp. 331-340, 2006.
31. Horowitz, S. B., Sheplak, M., Cattafesta III, L. N., and Nishida, T., "A MEMS Acoustic Energy Harvester," Journal of Micromechanics and Microengineering, Vol. 16, No. 9, pp. S174-S181, 2006.
32. Lee, H., Kang, D., and Moon, W., "A Micro-Machined Source Transducer for a Parametric Array in Air," The Journal of the Acoustical Society of America, Vol. 125, No. 4, pp. 1879-1893, 2009.
33. Olfatnia, M., Xu, T., Ong, L., Miao, J., and Wang, Z., "Investigation of Residual Stress and Its Effects on the Vibrational Characteristics

of Piezoelectric-Based Multilayered Microdiaphragms," Journal of Micromechanics and Microengineering, Vol. 20, No. 1, Paper No. 015007, 2009.

34. Griffin, B. A., Williams, M. D., Coffman, C. S., and Sheplak, M., "Aluminum Nitride Ultrasonic Air-Coupled Actuator," Journal of Microelectromechanical Systems, Vol. 20, No. 2, pp. 476-486, 2011.
35. Horowitz, S., Nishida, T., Cattafesta, L., and Sheplak, M., "Development of a Micromachined Piezoelectric Microphone for Aeroacoustics Applications," The Journal of the Acoustical Society of America, Vol. 122, No. 6, pp. 3428-3436, 2007.
36. Carlotti, G., Socino, G., Petri, A., and Verona, E., "Acoustic Investigation of the Elastic Properties of ZnO Films," Applied Physics Letters, Vol. 51, No. 23, pp. 1889-1891, 1987.
37. Bardaweel, H., Al Hattamleh, O., Richards, R., Bahr, D., and Richards, C., "A Comparison of Piezoelectric Materials for MEMS Power Generation," Proc. of the Sixth International Workshop on Micro and Nanotechnology for Power Generation and Energy Conversion Applications, pp. 207-210, 2006.

Min-Geon Kim
M.Sc. candidate in the Department of Mechanical Engineering, Seoul National University of Science and Technology. His research interest is in MEMS, Sensors and Resonant Devices.
E-mail: petrosskim@gmail.com

Ji-Seob Choi
B.Sc. candidate in the Department of Mechanical and Automotive Engineering, Seoul National University of Science and Technology. His research interest is in MEMS, Sensors, and Signal Process.
E-mail: giesoub93@gmail.com

Woo-Tae Park
Associate Professor in the Department of Mechanical and Automotive Engineering, Seoul National University of Science and Technology. His research interest is in MEMS, Sensors, and Medical Devices.
E-mail: wtpark@seoultech.ac.kr